ELSEVIER

Journal of Molecular Structure: THEOCHEM 818 (2007) 57–64

THEO CHEM

www.elsevier.com/locate/theochem

Theoretical study of N_2O_2 interaction with BaO(100) surface

Ricardo M. Ferullo [a,b,*], Silvia A. Fuente [b], María M. Branda [b], Norberto J. Castellani [b]

[a] Departamento de Química, Universidad Nacional del Sur, Av. Alem 1253, 8000 Bahía Blanca, Argentina
[b] Grupo de Materiales y Sistemas Catalíticos, Departamento de Física, Universidad Nacional del Sur, Av. Alem 1253, 8000 Bahía Blanca, Argentina

Received 21 December 2006; received in revised form 30 April 2007; accepted 1 May 2007
Available online 8 May 2007

Abstract

In this work, the adsorption of the NO dimer on BaO(100) was studied using the density functional theory (DFT). N_2O_2 interacts with the surface mainly in three different ways. In the more favoured orientation it adsorbs N-down forming a partially covalent bond with the surface with a charge electron delocalization over the adsorbate. In Tilted and O-down orientations, the dimer interacts in an electrostatic way with the surface Ba cations. The latter bonding modes are possible because an almost full electronic transfer from BaO to N_2O_2 takes place, producing the $N_2O_2^-$ species. In all these cases, the N–N distance of dimer decreases substantially due to the occupation of its $2b_1$ orbital, which has a very strong N–N bonding character. The results suggest that the formation of NO dimer should take place only at relatively high NO coverages.

Keywords: N_2O_2; NO dimer; BaO(100); Cluster model; NO_x storage

1. Introduction

The production of air pollutants such as hydrocarbons, carbon monoxide (CO) and nitrogen oxides (NO_x) generated by automobiles has become a serious environmental problem. For this purpose, the three way catalysts (TWC) were introduced to remove these gases in gasoline engines. However, an inconvenience is that the TWC are not able to reduce NO_x under an excess of oxygen. A possible solution comprises the storage concept, where the air–fuel ratio is altered between successive steps of oxygen excess and fuel excess mixtures [1]. During the first phase, the NO_x is trapped in a specific storage component of the catalyst. Then, in the second phase, it is regenerated and NO_x desorbs reacting with hydrocarbons and CO to produce CO_2, H_2O and N_2 on the surface of precious metals. The periodic sequence of these operating processes provides a high efficiency (more than 90%) for NO_x reduction. These new catalysts have two components: (i) a storage component, typically barium oxide (BaO) which acts as NO_x traps; (ii) an oxidizing and NO_x reducing component, typically Pt. In the past, some experimental studies were addressed to elucidate the NO_x storage mechanism [2,3].

Due to the great importance of the BaO surface as NO_x trap, some theoretical works have been performed to study the interaction of NO_x species with BaO surfaces by means of quantum-chemical methods [4–10]. In a series of papers, Broqvist et al. have modeled the possible mechanism for NO_2 storage using a periodic density functional theory (DFT) method [4,9,10]. On the other hand, Branda et al. have considered from DFT calculations [7] the NO and NO_2 adsorption on terrace, step and corner sites of a BaO surface. They found that while NO is covalently bonded to these sites, NO_2 oxidizes the surface and forms a stable NO_2^- species. For both NO and NO_2, the low-coordinated defects exhibit a much larger reactivity than the flat terrace.

The dimer of nitrogen monoxide (N_2O_2) is a possible intermediate in the reduction of NO in the gas phase [11] and in catalyzed reactions on surfaces [12–15]. At 70–90 K, N_2O is formed from N_2O_2 on the Ag(111) surface

* Corresponding author. Address: Departamento de Química, Universidad Nacional del Sur, Av. Alem 1253, 8000 Bahía Blanca, Argentina. Tel.: +54 291 4595141; fax: +54 291 4595142.
E-mail address: caferull@criba.edu.ar (R.M. Ferullo).

0166-1280/$ - see front matter © 2007 Elsevier B.V. All rights reserved.
doi:10.1016/j.theochem.2007.05.001

[12]. Morover, at much higher temperatures (in the range 400–600K) N_2O and N_2 are formed from N_2O_2 adsorbed on CaO and SrO [15]. The presence of this dimer on BaO surfaces was suggested from IR studies by Prinetto et al. [3]. Two intensive bands at 1375 and 1310 cm^{-1} observed upon NO adsorption on BaO/Al_2O_3 and $Pt–BaO/Al_2O_3$ samples were attributed to N–N stretching modes. However, these signals were no present after admission of a NO/O_2 mixture over the same samples.

Recently, the adsorption of NO dimer on MgO(100) was studied by performing cluster ab initio alculations [16,17]. *Cis*-N_2O_2 adsorbs very weakly over this surface and only on the magnesium cations. Its geometrical structure is characterized by a relatively long N–N distance of 1.81 Å, in comparison with typical N–N covalent bonds (≈1.1 Å). The interaction of NO molecules with the surface is strong only at defect sites and prevents the formation of dimers [16]. Cluster DFT calculations carried out for CaO(100) indicated that the adsorbed dimer adopts a geometry in which both NO monomers interact with the same five-coordinated oxygen, O_{5c}, and with the molecular plane being tilted towards the surface [18]. In this case, the value of N–N distance (1.63 Å) is shorter than on MgO(100). Very recently, the NO reaction on CaO(100) was investigated using ab initio molecular dynamics [19]. A two-step process was observed, producing first monovalent anionic dimers, $N_2O_2^-$, and later on, divalent anionic dimers, $N_2O_2^{2-}$. The formation of these species was possible at the expense of the oxidation of NO to NO^+. The final divalent anionic dimers could be the precursors for N_2O and N_2.

In the present work, the interaction of the NO dimer with the BaO(100) surface is studied from a theoretical point of view. For that purpose, the energies and electronic structure were determined by means of the DFT formalism. To our knowledge this is the first theoretical approach dedicated to the N_2O_2/BaO system. The main interest was to establish its inherent adsorption properties as a basis for other comparative and experimental works.

2. Computational method and cluster model

Our calculations were performed within the density functional theory (DFT) formalism, by using the ADF (Amsterdam Density Functional) package [20]. Computations were run using the local density approximation (LDA) with the Vosko–Wilk–Nusair functional. Generalized gradient (GGA) corrections are applied self-consistently through the Becke–Perdew (B88–P86) formulas [21]. For geometry optimization, the quasi Newton technique was employed.

It is generally recognized that the free neutral N_2O_2 molecule presents important correlation effects [22]. This observation can be related with the nearly degenerated $2\pi^*$ orbital of the weakly bounded NO monomers. The ground state is a singlet which adopts the symmetric-*cis* conformation [22,23]. Meanwhile this electronic configuration can not be predicted using the usually available DFT functionals, multireference-type methods attained the same electronic configuration as experiment [22]. When the negatively charged dimer $N_2O_2^-$ is considered, the situation is quite different. In this case, the molecule stabilizes noticeably and the N–N distance shortens about 0.8 Å with respect to the neutral dimer [24]. Concomitantly, the coupling between the $2\pi^*$ orbitals becomes stronger, producing a greater splitting of these energy levels. As a consequence, the electron correlation effects should be less important. In this case, the DFT results agree with high quality configuration interaction calculations, showing that the ground state for *cis* $N_2O_2^-$ has B_1 symmetry and that the first two excited states have A_1 and B_2 symmetries [24]. In fact, for this anion DFT methods correctly predict infrared frequencies, intensities and isotopic frequency ratios [25]. As it will be shown later, when N_2O_2 adsorbs on BaO it acquires a significant negative charge. Then, taking into account the above considerations, a study of the N_2O_2 adsorption within DFT formalism is expected to give accurate results. Moreover, an advantage of using DFT is that it correctly reproduces the electron affinity of N_2O_2, which is relevant when dealing with charged dimers [19].

The BaO(100) surface was represented by clusters of 42 atoms, $Ba_{21}O_{21}$, consisting of two layers. One of the clusters (cluster A) has a central oxygen atom in the first layer (with $Ba_{12}O_9$ composition). The other possible cluster (cluster B) has inverted the positions of barium and oxygen atoms with respect to cluster A. In Fig. 1, a view of cluster A has been displayed. As the other alkaline earth oxides, BaO have the rock salt (NaCl) structure. Several recent periodic supercell calculations indicate that the (100) surfaces of these oxides present very slight relaxations [8,26]. For this reason, the experimental bulk Ba–O distance of 2.76 Å was applied to generate the atomic coordinates. A Slater-type basis set was used for all the atoms. The inclusion of 1s levels in the selfconsistency produces negligible modifications of adsorption energies, showing that they are unrelevant to study the bonding of NO with BaO. Then, to accelerate the calculations the inner atomic states of oxygen and nitrogen (1s) were treated by the frozen-core approximation. The core of barium (1s2s2p3s3p3d4s4p4d)

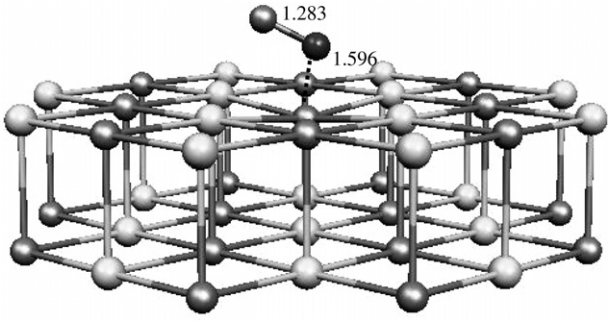

Fig. 1. Optimal geometry of NO molecule adsorbed on a surface O anion of BaO(100). The cluster is $Ba_{21}O_{21}$(A) and NO is N-down. Gray spheres: O; white spheres: Ba; black sphere: N.

was modeled using a relativistically corrected core potential created with the DIRAC utility of the ADF program. The DIRAC calculation is performed with the local density approximation (LDA); nevertheless, the fully relativistic Hamiltonian is employed, including spin–orbit coupling. The relativistic effects were considered by using the zero order regular approximation (ZORA) formalism [27]. The ZORA Hamiltonian splits into a spin–orbit term (regularized at the nucleus) and a remaining scalar relativistic part. By using this approximation, the atomic structure results are very near to that of full Dirac calculation. For example, the ionization potential for the elements of the sixth period are only 0.2% lower [27]. On the other hand, the ZORA constitutes an efficient way for the calculation of bonding energies in molecules, giving results which are very close to the experimental energies [28]. A triple-ζ plus polarization basis was used for the central 18 atoms (9 in the first layer and 9 in the second layer) and a double-ζ basis for the other atoms of each cluster. Based on the geometrical structures reported in the literature for N_2O_2 adsorption on MgO and CaO [17,18,29], five different bonding modes were considered. For time computing convenience, the geometry of the dimer was optimized keeping a specific symmetry (C_s or C_{2v}) of the dimer/oxide cluster system. Moreover, only the central atom in the first layer of cluster A or B was allowed to relax during the optimization process. In order to minimize the effects coming from the presence of cluster borders and for reproducing the Madelung potential at the adsorption site an embedding of point charges (PC's) was used. In doing so, a full ionic model have been assumed. The alkaline earth oxides with NaCl structure as MgO and BaO have a large ionic character. It was demonstrated that a large array having more than 200 PC's ($6\times6\times6$) is enough to predict the cohesive energy [30]. In our case, an array of about 800 PC's was employed ($10\times10\times8$). As the geometric optimization calculation with this kind of embedding was not implemented in the self-consistent cycles of the used ADF package, an indirect procedure was outlined. First, the adsorbate geometry was optimized using a $Ba_{21}O_{21}$ cluster. Then, we took this geometry and we made a single point calculation with the same cluster, but including an embedding of PC's. Such a procedure can be considered as adequate if we take into account the results obtained in other previous theoretical studies. For instance, in earlier works for the adsorption of small molecules (NH_3, CO, NO_x) on alkaline-earth oxides as MgO (see Ref. [31]) it was shown that the use of reasonably large clusters without considering an embedding of point charges gives optimized geometrical distances which differ at most $\approx$0.1 Å with respect the results with such embedding. On the other hand, more recently Grönbeck et al. have studied the NO_2 adsorption on BaO [10]. The NO_2/BaO system can be considered similar to the one analysed in this work because both NO_2 and N_2O_2 species have large electron affinities. The authors investigated size effects by comparing the results for $(BaO)_x$ clusters ($x = 4$, 6, 9, 12) with an extended BaO(1 0 0) surface. Adsorption energy and geometrical parameters values show a weak dependence on size. The value of NO_2 binding energy calculated for an extended BaO(1 0 0) surface is somewhat higher, indicating that the main effect of the long range electrostatic interactions is to stabilize the NO_2–BaO bond.

The adsorption energy E_{ads} was evaluated according to the following total energies difference: $E_{ads} = -E_T$(molecule/BaO cluster) + E_T(molecule) + E_T(BaO cluster). The importance of the basis set superposition error (BSSE) on the adsorption energy was evaluated for the largest and smallest adsorption energy values and we found that the absolute error is negligible, of about 0.05 eV. These results are in agreement with a previous work using the same basis sets [32]. Therefore, in the reported adsorption energy values this correction has not been included. The atomic net charge, spin density (SD) and overlap population (OP) values were calculated following the Mülliken scheme. The electronic structure of the adsorbate/surface bond was also analyzed from the projected density of states (PDOS) curves. They were computed by applying a 0.10 eV Lorentzian broadening to each energy eigenvalue of adsorbate/BaO system.

3. Results and discussion

3.1. NO adsorption on BaO(1 0 0)

From previous theoretical studies it was established that whereas the NO molecule physisorbs on terrace sites of MgO(1 0 0), it chemisorbs on CaO(1 0 0) and BaO(1 0 0) surfaces with adsorption energies of about 0.6 and 0.8 eV, respectively [7,18]. On the latter surfaces, the adsorption occurs on the O_{5c} site with an O_{5c}–N–O angle of about 110° and with the O_{5c}–N distance longer than the N–O one.

In Table 1, the main molecular and surface properties for NO adsorbed on the $Ba_{21}O_{21}$ (A) cluster are reported. The N–O distance stretches from 1.166 Å at gas phase to 1.283 Å when NO adsorbs on $Ba_{21}O_{21}$ (A) cluster. The NO molecule binds with the O_{5c} anion through the N atom, with an O_{5c}–NO distance of 1.6 Å (Fig. 1) and an adsorption energy of $\approx$1.0 eV. Additionally, it is tilted from the surface normal with an O–N–O_{5c} angle of 109.8°. The O atom of NO is equidistant from the two neighboring Ba cations, being the Ba–O distance equal to 2.93 Å, a value close to that of the bulk Ba–O (equal to 2.76 Å). For the sake of comparison, the results from other DFT calculations performed with an embedded Ba_9O_9 cluster are also exhibited in Table 1 [7]. Notice that the adsorption energies, distances, angles and spin densities values so calculated are in good agreement with our results.

The NO Mülliken net charge is negative, of nearly $-0.6e$ (Table 1). As the free NO molecule is neutral, this situation corresponds to an electronic charge transfer from the BaO surface. Indeed, the magnitude of negative charge of the nearest oxygen atom O_{5c} of BaO surface decreases by $\approx0.2e$. This electronic charge is localized along the NO

Table 1
Main adsorption properties for NO on BaO(100) surface

	$Ba_{21}O_{21}$(A)	Ba_9O_9; Ref. 7[b]
E_{ads} (eV)[a]	0.96	0.80
d(N–O) (Å)	1.283 (1.166)[c]	1.28
d(N–O_{5c})	1.596	1.53
d(O–Ba_{5c})	2.926	2.92
∠O_{5c} –N–O (°)	109.8	109.4
q(N) (e)	0.00 (+0.14)[c]	–
q(O)	−0.56 (−0.14)[c]	–
q(O_{5c})[d]	−0.94 (−1.17) [e]	–
q(Ba_{5c})[d]	+0.95 (+1.07)[e]	–
SD(N)	0.58 (0.72)[c]	0.63
SD(O)	0.32 (0.28)[c]	0.31
SD(O_{5c})	0.04	0.03
SD(Ba_{5c})	0.01	–
OP(N–O_{5c})	0.115	–
OP(N–O)	0.345 (0.479)[c]	–

[a] $E_{ads} = -E(NO/BaO) + E(BaO) + E(NO)$.
[b] B3LYP calculation. The Ba_9O_9 cluster is embedded by effective core potentials + PC's.
[c] The values in parentheses correspond to the free NO molecule.
[d] O_{5c} corresponds to the central O of the first layer and Ba_{5c} to its surface first nearest neighbours.
[e] The values in parentheses correspond to the bare $Ba_{21}O_{21}$ (A) cluster.

molecule because the net atomic charges of N and O modify by 0.14 and 0.42e, respectively, with respect to the free molecule. In this way, while the nitrogen atom is nearly neutral, the oxygen atom acquires a net atomic charge of −0.56e. The OP value of N–O_{5c} bond (≈0.1) is consistent with a partially covalent bond (Table 1). This result can be rationalized taking into account that a BaO to NO electron transfer takes place (see above). The latter yields a polarization of N–O_{5c} bond that moves the shared electron pair towards the N atom. Besides, the intramolecular N–O bond weakens, as it can be appreciated by the 28% decrease of OP(N–O) with respect to the free molecule value.

Comparing the spin density values for N and O atoms of adsorbed NO (Table 1), we observe that they are 19% lower and 14% higher, respectively, than those of free NO. However, the unpaired spin is distributed so that its larger fraction (about 50%) is localized on the nitrogen atom. Looking in more detail, we notice that a small portion of the spin (≈0.1 of SD) becomes delocalized on the BaO surface.

3.2. N_2O_2 adsorption on BaO(100)

In Table 2, the main molecular and surface properties for N_2O_2 adsorbed on BaO(100) are summarized. Five different bonding modes were considered taking into account three different types of interaction with the surface: (i) N-down: the N atom is directly linked with a surface O^{2-} site. In this case, the dimer atoms can move only in two different normal planes (Fig. 2): one intersecting the surface O^{2-} anions (N-down (I)) and the other intersecting the surface O^{2-}–Ba^{2+}– O^{2-} ions (N-down (II)); (ii) tilted: the N atoms interact with the an O^{2-} site and the O atoms are tilted towards the Ba^{2+} sites (Fig. 3); (iii) O-down: the O atoms point to the surface and link with the Ba^{2+} site (Fig. 4). In this case, as for N-down modes, the adsorbate molecule

Table 2
Main adsorption properties for N_2O_2 on BaO(100)

	N-down (I) (Fig. 2)	N-down (II) (Fig. 2)	Tilted (Fig. 3)	O-down (I) (Fig. 4)	O-down (II) (Fig. 4)
M[a]	1	1	3	3	3
E'_{ads}(eV)[b]	0.79	0.68	0.51	0.37	0.35
E_{dim}[c]	0.62	0.41	0.06	−0.21	−0.26
q(N) (e)	0.44[d]/−0.01	0.41[d]/0.01	0.08	0.10	0.10
q(O)	−0.66[d]/−0.49	−0.62[d]/−0.50	−0.52	−0.42	−0.42
q(N_2O_2)	−0.72	−0.70	−0.90	−0.64	−0.64
q(O_{5c})	−0.90 (−1.17)[e]	−0.91	−1.06	−1.14 (−1.16)[f]	−1.14
q(Ba_{5c})	+0.96(+1.07)[e]	+0.96	+0.99	+0.80(+0.75)[f]	+0.78
SD(N)	–	–	0.17	0.23	0.24
SD(O)	–	–	0.25	0.35	0.36
SD(N_2O_2)	–	–	0.84	1.16	1.20
SD(O_{5c})	–	–	0.36	0.10	0.10
SD(Ba_{5c})	–	–	0.00	0.00	0.00
OP(N–O_{5c})	0.339	0.341	0.008	–	–
OP(O–Ba_{5c})	–	–	0.114	0.095	0.094
OP(N–N)	0.660	0.761	0.606	0.613	0.610
OP(N–O)	0.460[d]/0.490	0.502[d]/0.491	0.432	0.441	0.446

[a] M means for multiplicity.
[b] Adsorption energy per NO molecule: $E'_{ads} = 1/2[-E(N_2O_2/BaO) + E(BaO) + 2E(NO)]$.
[c] $E_{dim} = -E(N_2O_2/BaO) + E(NO/BaO) + E(NO)$.
[d] N and O atoms closest to the surface.
[e] The values in parentheses correspond to the bare $Ba_{21}O_{21}$ (A) cluster.
[f] The values in parentheses correspond to the bare $Ba_{21}O_{21}$ (B) cluster.

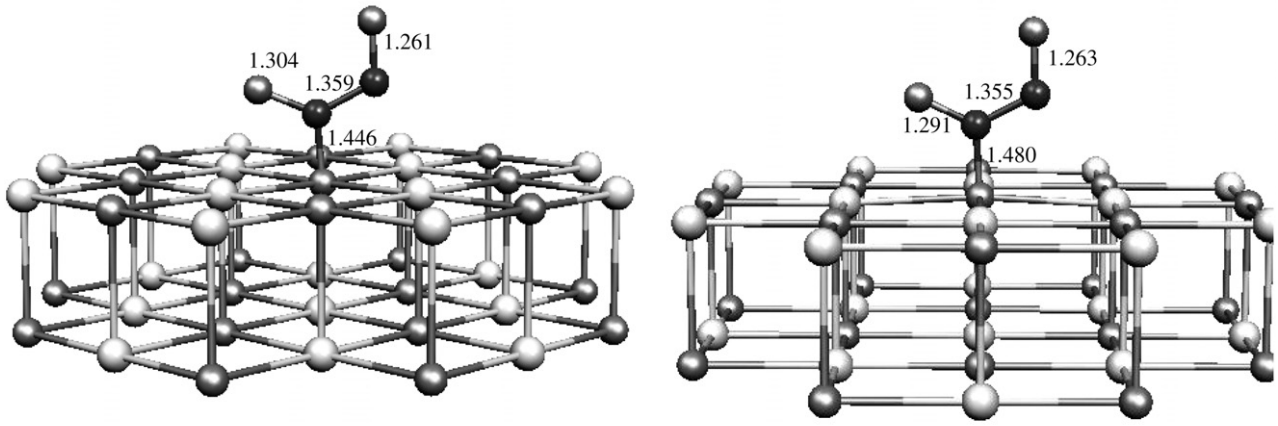

Fig. 2. Optimal geometries of N_2O_2 adsorbed N-down on a surface O anion of BaO(100). The cluster is $Ba_{21}O_{21}$(A). Left: structure I. Right: structure II. Gray spheres: O; white spheres: Ba; black spheres: N.

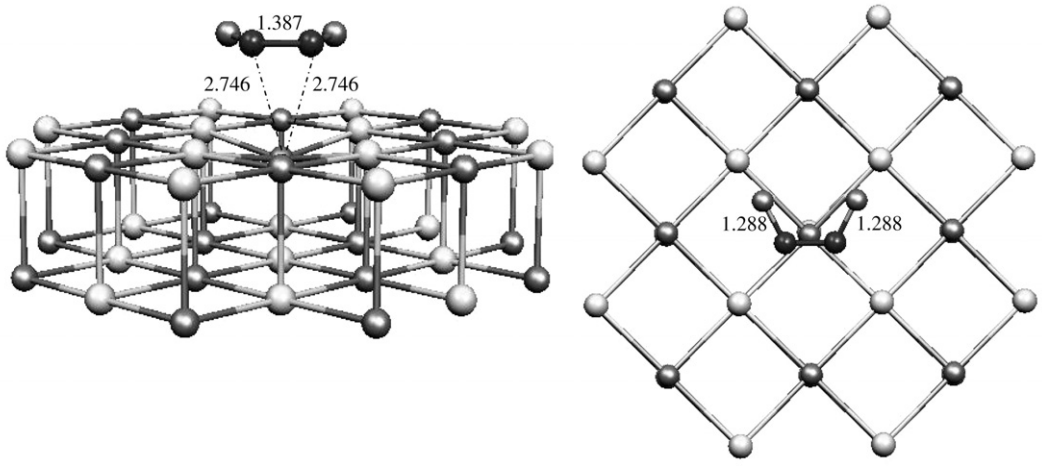

Fig. 3. Optimal structure of N_2O_2 adsorbed in Tilted orientation on a surface O anion of BaO(100). The cluster is $Ba_{21}O_{21}$(A). Gray spheres: O; white spheres: Ba; black spheres: N.

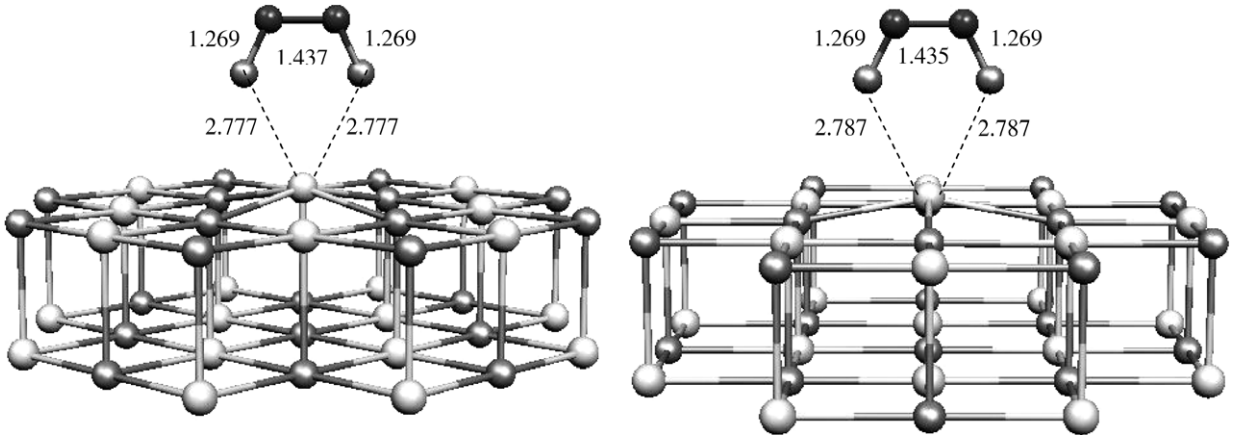

Fig. 4. Optimal structures of N_2O_2 adsorbed O-down on a surface Ba cation of BaO(100). The cluster is $Ba_{21}O_{21}$(B). Left: structure I. Right: structure II. Gray spheres: O; white spheres: Ba; black spheres: N.

is geometrically constrained in two different normal planes (O-down (I) and (II)).

For all the geometrical structures, both triplet and singlet electronic configurations were examined. For N-down, the singlet was the most stable configuration, being the triplet 1.3 eV less stable. Conversely, for Tilted and O-down orientations, the triplet was the most favoured electronic configuration, being only 0.2 eV more stable than the singlet (Table 2).

The stability of the adsorbed dimer was evaluated by means of the adsorption energies expressed per NO monomer. They are defined as $E'_{ads} = 1/2[-E(N_2O_2/BaO)+ E(BaO) + 2E(NO)]$. The N-down modes are the most favoured with a mean adsorption energy of 0.73 eV (Table 2). The other types of adsorption, Tilted and O-down, present mean E'_{ads} values of 0.51 and 0.35 eV, respectively. The N–N intramolecular distances (Figs. 2–4) are in the range of 1.35–1.44 Å for all the adsorbed structures. These values are similar to that calculated for free $N_2O_2^-$ (1.45 Å) but significantly shorter than for neutral N_2O_2 dimer (which is ≈ 2.0 Å at DFT level [33] and 2.24 Å from experimental measurements [23]). Concerning the interatomic distances between the adsorbate molecule and the oxide surface, whereas the N–O_{5c} distance is about 1.4 Å for N-down, it is close to 2.7 Å for tilted and for O-down.

The N-down modes can be viewed as the result of the interaction between a NO molecule at gas phase with a pre-adsorbed NO. In fact, the geometry for the NO molecule of dimer which is closer to the surface is analogous than that of the isolated adsorbed NO. For N-down (I), the O–N–O_{5c} angle varies from 109.8° when the single NO is adsorbed, to 117.0° when the dimer is produced. On the other hand, the N–O_{5c} and O–Ba_{5c} distances shorten from 1.60 to 1.45 Å, and from 2.93 to 2.80 Å, respectively. In order to study this interaction with more detail, the dimer formation energy was defined as $E_{dim} = -E(N_2O_2/BaO) + E(NO/BaO) + E(NO)$. The corresponding values are summarized in Table 2. While this dimerization process is favoured for N-down, it is not favoured for O-down. Besides, it is very weakly favoured for Tilted adsorption. The calculated value of E_{dim} for N-down (I) geometry (0.62 eV) is smaller than that for the NO adsorption on a clean BaO surface (0.96 eV). As a consequence, a NO molecule prefers to adsorb on a clean surface rather than on a pre-adsorbed NO. Similar results were found for the NO dimer formation on CaO(1 0 0) by Di Valentin et al. [18]. However, as it was clearly discussed by these authors, the adsorbate-adsorbate interaction is usually repulsive and, then, at a relatively high coverage it should be a major trend to form NO dimers. To check this point, a calculation adsorbing two NO molecules on two adjacent O^{2-} sites was performed. The result indicates that this situation is 0.17 eV less stable with respect to two separated NO ad-molecules.

Another way to study the relative stability of the dimer can be achieved by comparing the adsorption energy values for NO and N_2O_2 (Tables 1 and 2). The adsorption energy value is 1.58 eV (two times the E'_{ads} value of Table 2), when two molecules adsorb simultaneously on a O^{2-} site of BaO for N-down (I) geometry. By comparison, the same energy is 1.92 eV when two molecules adsorb separately. Thus, the adsorbed dimer is less stable by 0.34 eV with respect to two separated NO molecules. For CaO, a similar calculation gives an energy difference of 0.51 or 0.65 eV (depending on the type of embedding) [18]. These results show that there is a somewhat higher trend to form NO dimers on BaO than on CaO. In fact, taking into account the great ability of dimer to take an electron, an increasing facility to form N_2O_2 on alkaline-earth-metal oxides when going from MgO to BaO is expected, because in this way the surface basicity also increases [7]. Thus, among these oxides, BaO should be considered the best catalyst for NO reduction to N_2 or N_2O because it produces easily intermediate NO dimers. In these species a strong N–N bond is present, an obvious requirement for the nitric oxide reduction.

The N_2O_2 Mulliken net charge is negative in all the cases, ranging from −0.65 and −0.70*e* for O-down and N-down, respectively, to −0.90*e* for Tilted (Table 2). This negative charge corresponds, as in the case of NO molecule, to an electronic charge transfer from the BaO surface. Its amount is ≈0.1 to 0.3*e* greater than for the monomer. Notice that for N-down modes, the O_{5c} atom and its surrounding Ba_{5c} atoms give 0.7*e* to N_2O_2, just the electronic charge value taken by N_2O_2. This well localized character of charge transfer can be related to the relative short N_2O_2–BaO distance, as a consequence of the formation of a partially covalent bond between adsorbed molecule and surface (see later). If we consider the cases of Tilted and O-down orientations, the nearest O and Ba ions of the BaO surface release only 0.4 and 0.1*e*, respectively. Then, the surface region that brings its electronic charge to N_2O_2 is spatially more extended. Notice that for N-down this charge becomes unevenly distributed along the N_2O_2 molecule, while in the Tilted and O-down modes the electronic charge is distributed rather homogeneously both on N and O atoms.

Regarding the OP values, those of the N–O_{5c} bond for the N-down modes (≈0.34) indicate a significant covalent contribution, which is stronger than in the case of the monomer adsorption (≈0.11; see Table 1). On the other hand, the OP(N–O_{5c}) and the OP(O–Ba_{5c}) values for Tilted and O-down (≈0.0 and ≈0.1, respectively) are consistent with the formation of ionic bonds. The same consequence can be inferred from the OP(O–Ba_{5c}) values for Tilted adsorption (≈0.11). In fact, for Tilted and O-down orientations, the NO dimer can be viewed as a $N_2O_2^-$ species which interacts electrostaticaly with the neighbouring Ba cations. Indeed, the distance between the O atom of dimer with the closest Ba^{2+} is 2.78 and 2.76 Å for O-down and Tilted modes, respectively, essentially the same than that for bulk Ba^{2+}–O^{2-} (2.76 Å). Besides, the OP(N–N) values are similar to that for the free $N_2O_2^-$ species (0.645).

Moreover, because for the Tilted and O-down adsorption geometries the electronic configuration corresponds

to a triplet, the more relevant spin densities of N_2O_2 have been evaluated (Table 2). The spin is homogeneously distributed in this molecule, with a SD value of 0.15–0.25 on the N atoms and of 0.25–0.35 on the O atoms. The greater calculated values are for the O-down structures. The spin density accumulated on N_2O_2 molecule ranges from 0.80 to 1.20; therefore, the rest of spin density becomes localized on the BaO substrate.

Besides, the electronic structure for the N_2O_2/BaO system has been analyzed considering the projected density of states (PDOS) for the most important valence molecular orbitals of N_2O_2. In Figs. 5 and 6, the calculated PDOS of $7a_1$ and $2b_1$ molecular orbitals for different types of adsorption are displayed. The one electron $7a_1$ and $2b_1$ orbitals of neutral N_2O_2 (the HOMO and the LUMO, respectively) are formed by coupling the $2\pi^*$ orbitals of NO monomers. A sketch of these orbitals is also depicted in Fig. 5. These orbitals are characterized by a bonding N–N interaction, and an antibonding N–O interaction. For N-down (I) (Fig. 5), the N_2O_2 $7a_1$ molecular orbital undergoes a high degree of coupling with the O(p) orbitals than the $2b_1$ one. This can be explained because the $7a_1$ orbital has a lobe located at the N atom that points directly to the p orbitals of the surface O anion. Additionally, the $2b_1$ orbital lies below the Fermi level and, as a consequence, this orbital gains two electrons. For the dimer adsorbed in the Tilted orientation (Fig. 6), the hybridization is less significant showing an interaction mainly ionic with the surface. For O-down, the PDOS curves is very similar (not shown). In both cases, whereas the $2b_1$ orbital gains one electron, the $7a_1$ one remains with two electrons, thus resembling the electronic configuration for free $N_2O_2^-$ ($\ldots 6b_2^2 2b_1^1 7a_1^2$).

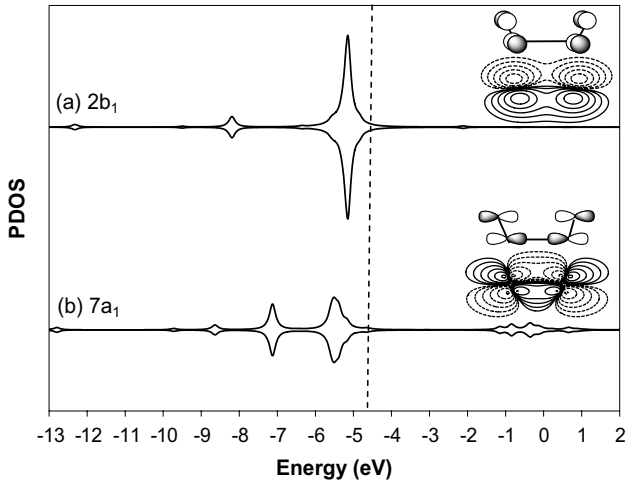

Fig. 5. PDOS of $7a_1$ and $2b_1$ molecular orbitals for dimer N-down (I) adsorption. The vertical dashed line corresponds to the Fermi level. In the insets, the pictures of the one electron HOMO ($7a_1$) and LUMO ($2b_1$) levels for free neutral N_2O_2 are shown. The counter diagram of the $2b_1$ molecular orbital is plotted at 0.4 Å above the molecular plane.

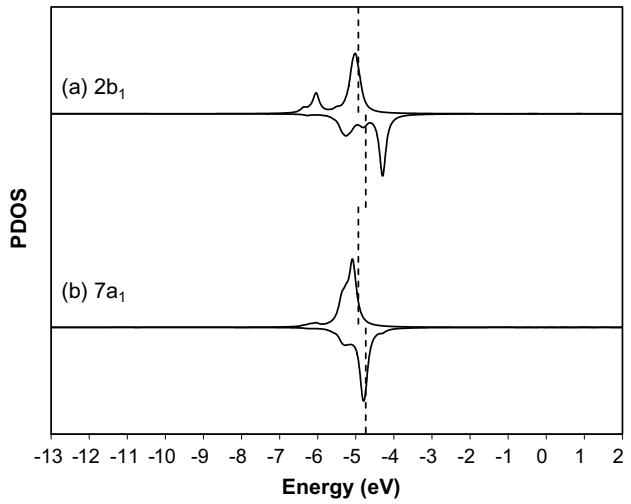

Fig. 6. PDOS of $7a_1$ and $2b_1$ molecular orbitals for dimer Tilted adsorption. The vertical dashed line corresponds to the Fermi level.

4. Conclusions

In the most stable geometry, the NO dimer interacts with the surface accordingly to an N-down orientation, forming a partially covalent bond with the surface with a great delocalization over the adsorbate. Two other types of adsorption were found, Tilted and O-down, where an ionic bond is produced with the surface Ba cations. The latter bonding modes occur due to a significant electron transfer from BaO to N_2O_2, producing a $N_2O_2^-$ species. In all cases, the N–N distance of the dimer decreases substantially due to the occupation of the $2b_1$ orbital, which has a very strong N–N bonding character.

The NO molecule prefers to adsorb on a clean surface rather than on a pre-adsorbed NO. Moreover, due to the adsorbate-adsorbate repulsive interaction, the formation of the NO dimer should take place only at relatively high NO coverages.

The PDOS of the $7a_1$ molecular orbital for the N-down type of adsorption shows a high degree of coupling with the O(p) orbitals of the oxide. The $2b_1$ orbital lies below the Fermi level and, as a consequence, this orbital gains two electrons. For the Tilted and O-down modes, the PDOS profiles show an interaction mainly ionic with the surface. In both cases, whereas the $2b_1$ orbital gains one electron, the $7a_1$ one remains with two electrons; thus, the dimer electronic configuration resembles that of free $N_2O_2^-$ species.

Acknowledgements

The authors acknowledge the financial support of Universidad Nacional del Sur, CONICET and ANPCyT of Argentina.

References

[1] W. Bögner, M. Krämer, B. Krutzsch, S. Pischinger, D. Voigtländer, G. Wenninger, F. Wirbeleit, M.S. Brogan, R.J. Brisley, D.E. Webster, App. Catal. B 7 (1995) 153;
N. Takahashi, H. Shinjoh, T. Iijima, T. Suzuki, K. Yamazaki, K. Yokota, H. Suzuki, N. Miyoshi, S. Matsumoto, T. Tanizawa, T. Tanaka, S. Tateishi, K. Kasahara, Catal. Today 27 (1996) 63.

[2] H. Mahzoul, J.F. Brilhac, P. Gilot, App. Catal. B 20 (1999) 47;
Y. Chi, S.S.C. Chuang, J. Phys. Chem. B 104 (2000) 4673;
E. Fridell, H. Persson, B. Westerberg, L. Olsson, M. Skoglundh, Catal. Lett. 66 (2000) 71;
L. Olsson, E. Fridell, M. Skoglundh, B. Andersson, Catal. Today 73 (2002) 263;
N.W. Cant, M.J. Patterson, Catal. Today 73 (2002) 271;
J. Despres, M. Koebel, O. Kröcher, M. Elsener, A. Wokaun, App. Catal. B 43 (2003) 389;
Ch. Sedlmair, K. Seshan, A. Jentys, J.A. Lercher, J. Catal. 214 (2003) 308.

[3] F. Prinetto, G. Ghiotti, I. Nova, L. Lietti, E. Tronconi, P. Forzatti, J. Phys. Chem. B 105 (2001) 12732.

[4] P. Broqvist, I. Panas, E. Fridell, H. Persson, J. Phys. Chem. B 106 (2002) 137.

[5] E.J. Karlsen, L.G.M. Pettersson, J. Phys. Chem. B 106 (2002) 5719.

[6] E.J. Karlsen, M.A. Nygren, L.G.M. Pettersson, J. Phys. Chem. A 106 (2002) 7868.

[7] M.M. Branda, C. Di Valentin, G. Pacchioni, J. Phys. Chem. B 108 (2004) 4752.

[8] W.F. Schneider, J. Phys. Chem. B 108 (2004) 273.

[9] P. Broqvist, I. Panas, H. Grönbeck, J. Phys. Chem. B 109 (2005) 15410.

[10] H. Grönbeck, P. Broqvist, I. Panas, Surf. Sci. 600 (2006) 403.

[11] J. Wang, L. Jia, E.J. Anthony, AIChE J. 49 (2003) 277.

[12] W.A. Brown, P. Gadner, D.A. King, J. Phys. Chem. 99 (1995) 7065.

[13] R. Ramprasad, K.C. Hass, W.F. Schneider, J.B. Adams, J. Phys. Chem. B 101 (1997) 6903.

[14] S. Haq, A. Carew, R. Raval, J. Catal. 221 (2004) 204.

[15] Y. Yanagisawa, Appl. Surf. Sci. 100 (1996) 256.

[16] C. Di Valentin, G. Pacchioni, M. Chiesa, E. Giamello, S. Abbet, U. Heiz, J. Phys. Chem. B 106 (2002) 1637.

[17] X. Lu, X. Xu, N. Wang, Q. Zhang, J. Phys. Chem. B 103 (1999) 5657.

[18] C. Di Valentin, A. Figini, G. Pacchioni, Surf. Sci. 556 (2004) 145.

[19] C. Di Valentin, G. Pacchioni, M. Bernasconi, J. Phys. Chem. B 110 (2006) 8357.

[20] ADF 2003.01, Vrije Universiteit, Amsterdam, The Netherlands.

[21] A.D. Becke, Phys. Rev. A 38 (1988) 3098;
J.P. Perdew, Phys. Rev. B 33 (1986) 8822.

[22] M. Tobita, S. Ajith Perera, M. Musial, R.J. Bartlett, M. Nooijen, J.S. Lee, J. Chem. Phys. 119 (2003) 10713.

[23] S.G. Kukolich, J. Am. Chem. Soc. 104 (1982) 4715.

[24] A. Snis, I. Panas, Chem. Phys. 221 (1997) 1.

[25] L. Andrews, M. Zhou, S.P. Willson, G.P. Kushto, A. Snis, I. Panas, J. Chem. Phys. 109 (1998) 177.

[26] P. Broqvist, H. Grönbeck, I. Panas, Surf. Sci. 554 (2004) 262;
N.V. Skorodumova, K. Hermansson, B. Johansson, Phys. Rev. B 72 (2005) 125414.

[27] E. van Lenthe, E.J. Baerends, J.G. Snijders, J. Chem. Phys. 101 (1994) 9783.

[28] P.H.T. Philipsen, E. van Lenthe, J.G. Snijders, E.J. Baerends, Phys. Rev. B 56 (1997) 13556.

[29] A. Snis, I. Panas, Surf. Sci. 412/413 (1998) 477.

[30] Y. Kawamura, H. Nakai, Chem. Phys. Lett. 410 (2005) 64.

[31] Y. Nakajima, D.J. Doren, J. Chem. Phys. 105 (1996) 7753;
A.G. Pelmenschikov, G. Morosi, A. Gamba, S. Coluccia, J. Phys. Chem. B 102 (1998) 2226;
M. Miletic, J.L. Gland, K.C. Hass, W.F. Schneider, J. Phys. Chem. B 107 (2003) 157.

[32] A. Rosa, A.W. Ehlers, E.J. Baerends, J.G. Snijders, G. te Velde, J. Phys. Chem. 100 (1996) 5690.

[33] H.A. Duarte, E. Proynov, D.R. Salahub, J. Chem. Phys. 109 (1998) 26.